NJC

New Journal of Chemistry

A journal for new directions in chemistry

www.rsc.org/njc

Volume 35 | Number 9 | September 2011 | Pages 1761–1908

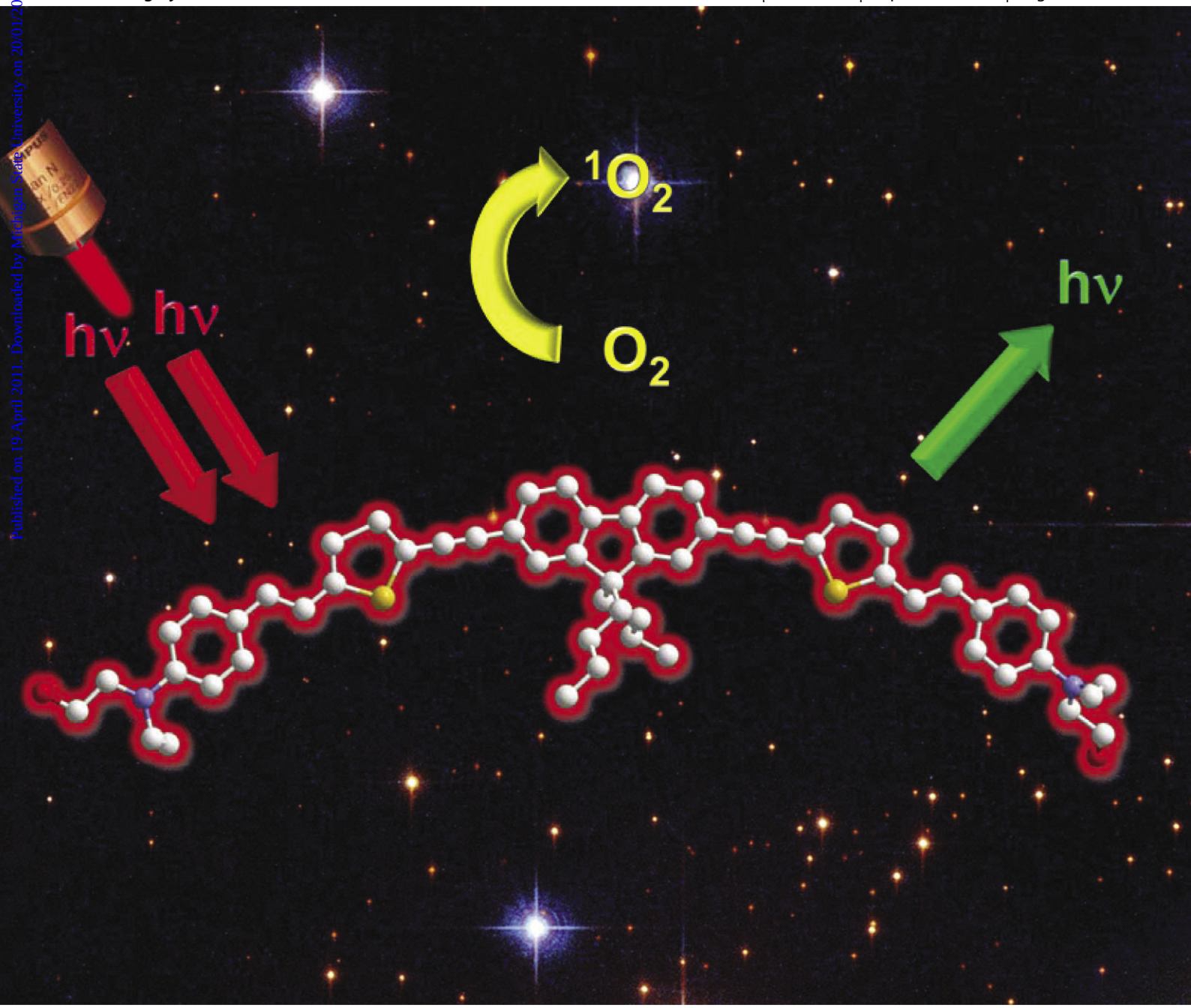

ISSN 1144-0546

RSC Publishing

NJC

View Article Online
Dynamic Article Links

Cite this: *New J. Chem.*, 2011, **35**, 1771–1780

www.rsc.org/njc

PAPER

Banana-shaped biphotonic quadrupolar chromophores: from fluorophores to biphotonic photosensitizers†

Cédric Rouxel,[ab] Marina Charlot,[ab] Youssef Mir,[ab] Céline Frochot,[c] Olivier Mongin*[ab] and Mireille Blanchard-Desce*[ab]

Received (in Montpellier, France) 27th January 2011, Accepted 25th March 2011
DOI: 10.1039/c1nj20073a

This study aims at designing *dual-role* biphotonic chromophores that could be used for photodynamic therapy (PDT) while maintaining some fluorescence in order to locate them, thus allowing selective irradiation of cancer cells when combined with targeting. Quadrupolar two-photon absorbing fluorophores were synthesized from the symmetrical functionalization of a fluorene core bearing elongated conjugated rods made from arylene–vinylene or arylene–ethynylene building blocks in order to test modifications which could increase singlet oxygen production ability while retaining some fluorescence and high two-photon absorption (TPA) cross-sections in the biological spectral range of interest. All chromophores show a polar emissive excited state whose dipole moment is highly dependent on the nature of the conjugated linker. Interestingly, the largest TPA responses in the NIR region as well as singlet oxygen quantum yield are correlated with the smallest dipole moment of the emissive excited-state. The molecular optimization study led to a multifunctional biphotonic chromophore combining high TPA cross-sections in the whole spectral range of interest (700–900 nm), reasonable singlet oxygen production efficiency, significant remaining fluorescence, and alcohol end-groups for further covalent grafting. This compound offers thus interesting potentialities for highly selective spatially-resolved two-photon PDT by incorporation in nanostructures.

Introduction

Molecular two-photon absorption (TPA) has gained increasing attention over recent years,[1–4] in relation with the wide-ranging applications it offers, such as microfabrication,[5–7] 3D optical data storage,[8,9] optical power limiting,[10,11] two-photon laser scanning microscopy[12,13] or photodynamic therapy[14–17] (PDT). Most of these applications require both pulsed sources (to increase the probability of this nonlinear process) *i.e.* femtosecond, picosecond, or possibly nanosecond lasers and chromophores exhibiting very high TPA cross-sections (intense but also broad TPA bands are highly desirable due to the versatility these offer in terms of laser sources), allowing either more efficient excitation or decrease of the excitation intensity (use of less expensive laser sources). This also offers a number of advantages for biological or biomedical applications, including the ability for highly selective excitation in biological media, intrinsic three-dimensional resolution, and reduction of photodamage by using lower excitation intensities. Depending on the targeted applications, TPA chromophores have to fulfil different requirements: molecular engineering depends on the desired application, in terms of spectral range and specific additional features. For instance, in the case of biological imaging, high fluorescence quantum yields, photostability and absence of toxicity as well as very large TPA cross-sections in the biological spectral window (700–1100 nm) are required.[18–20] Such large TPA cross-sections are also required for photodynamic therapy in addition to high singlet oxygen production quantum yield or reactive oxygen species sensitization (harmful to cancer cells).[3,21] Hence biphotonic chromophores (*i.e.* chromophores having very large TPA cross-sections) suitable for PDT or imaging would have different excited state outcomes: fluorescence (for imaging applications) or redox behavior or sensitization of oxygen for PDT. The present work aims at designing *dual-role* biphotonic chromophores that could be used for PDT while maintaining some fluorescence in order to locate them, thus allowing selective irradiation of cancer cells when combined with targeting. Such chromophores should thus combine significant fluorescence and singlet oxygen quantum yields while having very large TPA cross-sections in the biological spectral window.

[a] *CNRS, Chimie et Photonique Moléculaires (UMR 6510), 263 avenue du Général Leclerc, 35042 Rennes, France. E-mail: mireille.blanchard-desce@univ-rennes1.fr, olivier.mongin@univ-rennes1.fr*
[b] *Université de Rennes 1, UMR 6510, Campus de Beaulieu, Bâtiment 10A, Case 1003, 35042 Rennes, France*
[c] *LRGP UPR 3349, Nancy-Université, CNRS, 1 rue Grandville, BP 20451, F-54001 Nancy, France*

† Electronic supplementary information (ESI) available: Photophysical properties, emission spectra and Perrin plots of compounds **Q1**, **Q2** and **Q′2** in different solvents. See DOI: 10.1039/c1nj20073a

Most of the one-photon photosensitizers are porphyrin derivatives; however, single porphyrins have low TPA cross-sections in the spectral range of interest (15 GM for tetraphenylporphine).[22] Giant TPA cross-sections can be obtained with expanded porphyrins,[23,24] diyne porphyrin dimers,[25] fused porphyrin dimers,[26] porphyrin arrays[27] or supramolecular assemblies,[25,28] however, at the expense of a definite decrease of the fluorescence quantum yield (if not suppression) and residual one-photon absorption overlapping with the TPA band. Indeed the one-photon resonance enhancement at the origin of the giant TPA values results in a loss of some of the advantages resulting from selective TPA, in particular the 3D resolution. In this context, our aim was to develop alternative two-photon fluorescent photosensitizers based on banana-shaped quadrupolar systems. We have previously shown that such derivatives can combine very large TPA cross-sections and high fluorescence quantum yields.[29–35] Among others, this approach led to membrane markers for two-photon cellular imaging,[30,36] but also to nanodots[37–39] with outstanding two-photon brightness as "soft" biocompatible substitutes to toxic quantum dots for *in vivo* imaging in living animals.[38] Based on these results, our purpose was to investigate structural variation of the quadrupolar systems, in order to increase intersystem crossing *while* maintaining significant fluorescence quantum yields in order to obtain biphotonic sensitizers that retain fluorescence to allow *in vivo* monitoring and subsequent localized irradiation.

Ogilby and coworkers[40–42] have implemented a successful strategy based on the adjunction of heavy atoms such as bromine on a quadrupolar backbone. This leads to efficient intersystem crossing and singlet oxygen generation quantum yields but concomitantly to vanishing fluorescence. We herein explore an alternative approach by modifying aromatic building blocks in the conjugated system (replacing phenylene units by thienylene units, in order to increase intersystem crossing), and by adding terminal grafting moieties. Such moieties could be of interest for conjugation of photosensitizers with hydrophilic targeting moieties, such as peptides[43–45] or folic acid.[46,47] This would provide an expeditious way to provide water-solubility. Alternatively, in lieu of direct conjugation, terminal grafting moieties are also intended for covalent anchoring of the photosensitizers within the matrix of silica nanoparticles[48] or the addition of shielding dendritic branches.[38,49] Such routes would allow isolating the lipophilic chromophores from the water environment, in particular from the deleterious effects of water on TPA[50] but also on the singlet oxygen and fluorescence quantum yields.[38] In addition, nanostructures such as nanoparticles or dendrimers offer high flexibility for further surface-functionalization with hydrophilic targeting moieties.[48,51]

Results and discussion

Design

Four biphotonic quadrupolar chromophores have been studied in the present work (Chart 1). Model compounds **Q1** and **Q2** were chosen as lead compounds, since they combine photostability, in relation with triple bonds in the conjugated system, broad and intense TPA bands in the 700–900 nm range, as well as high fluorescence quantum yield (Φ_f).[35] Molecule **Q2** exhibits a larger TPA cross-section (σ_2) than **Q1**, but a lower fluorescence quantum yield, which leads to a similar two-photon brightness ($\sigma_2\Phi_f$) for both molecules. However for the targeted application (fluorescence + PDT), **Q2** could be more efficient than **Q1** ($\sigma_2\Phi_\Delta$ being the figure of merit for the singlet oxygen production, where Φ_Δ is the singlet oxygen quantum yield) if increase of intersystem crossing is responsible for the decrease of the fluorescence quantum yield. Compound **Q′2**, a functionalized analogue of **Q2**

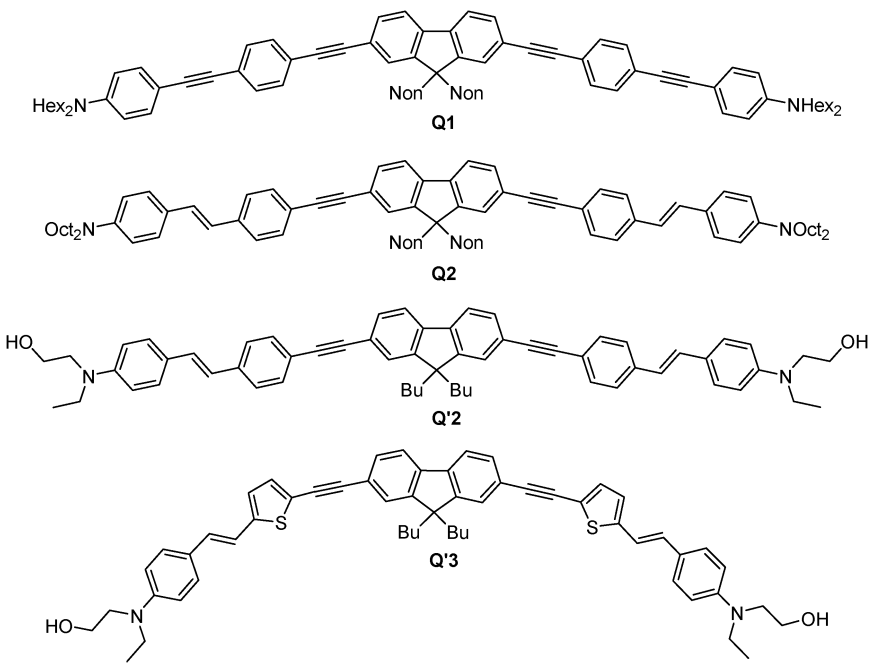

Chart 1 Chemical structures of **Q1**, **Q2**, **Q′2** and **Q′3** (Non = *n*-nonyl, Bu = *n*-butyl).

possessing terminal grafting moieties, has also been synthesized, in order to evaluate the potential influence of these non-conjugated auxiliary groups on the photophysical properties, *via* environmental effect. Finally **Q′3**, in which phenylene units have been replaced by thienylene units in the conjugated system, has also been prepared. According to the essential-state model[52,53] such a replacement is expected to lead to TPA enhancement, but it could also increase inter-system crossing,[54] which could in turn facilitate singlet oxygen production.

Synthesis

Quadrupolar chromophores **Q1** and **Q2** were synthesized according to the procedures reported in ref. 35. The synthesis of chromophores **Q′2** and **Q′3** is described in Scheme 1. The fluorene core **1c** was obtained from 9,9-dibutyl-2,7-diiodo-9*H*-fluorene (**1a**)[55] by means of a twofold Pd(II)-catalyzed cross-coupling with 2-methyl-3-butyn-2-ol, followed by base-promoted deprotection of the resulting intermediate **1b**. Double Sonogashira coupling of **1c** with 4-bromobenzaldehyde (**2**) afforded bis-aldehyde **3**. In contrast, analogous reaction with 5-bromothiophene-2-carboxaldehyde failed in our hands and this compound had to be replaced by the corresponding iodo derivative **5**,[56] to afford **6** very efficiently. Wittig condensations of **3** and **6** with phosphonium salt **4**[57] led to chromophores **Q′2** and **Q′3**, respectively, as single (*E*,*E*)-stereoisomers. It should be noted that protection of the alcohol function of **4** proved unnecessary.

Photophysical properties

One-photon absorption (OPA) and photoluminescence properties. Table 1 and Fig. 1 show, respectively, the compared photophysical properties and the absorption/emission spectra of compounds **Q1**, **Q2**, **Q′2** and **Q′3** in toluene. All chromophores present an intense absorption band from the near UV to the blue visible range. The maximum molar extinction coefficients of the four chromophores gathered in Table 1 are very large and all the oscillator strengths are much higher than 1, concomitantly with large full widths at half maximum. On one hand fluorescence quantum yields of **Q1**, **Q2** and **Q′2** are relatively high, ranging between 0.6 and 0.8, which is of interest for imaging applications. On the other hand, compound **Q′3** shows a lower fluorescence quantum yield indicative of the onset of non-radiative deactivation processes competing with fluorescence emission.

As expected, substitution of a triple bond (compound **Q1**) by a double bond (compound **Q2**) in the conjugated path induces a bathochromic shift of both absorption and emission bands (Fig. 1), in agreement with improved electronic delocalization. As well as being more transparent, compound **Q1** is also more fluorescent than its analogue **Q2**, this effect being related mostly to a smaller non-radiative decay rate due to reduced conformational flexibility. Replacing the long lipophilic chains on the amino donating end groups (compound **Q2**) by grafting moieties (compound **Q′2**) induces a slight blue shift of the absorption band and reductions of both the fluorescence quantum yield (due to a larger non-radiative decay rate) and anisotropy (in relation with the smaller size). Finally, replacement

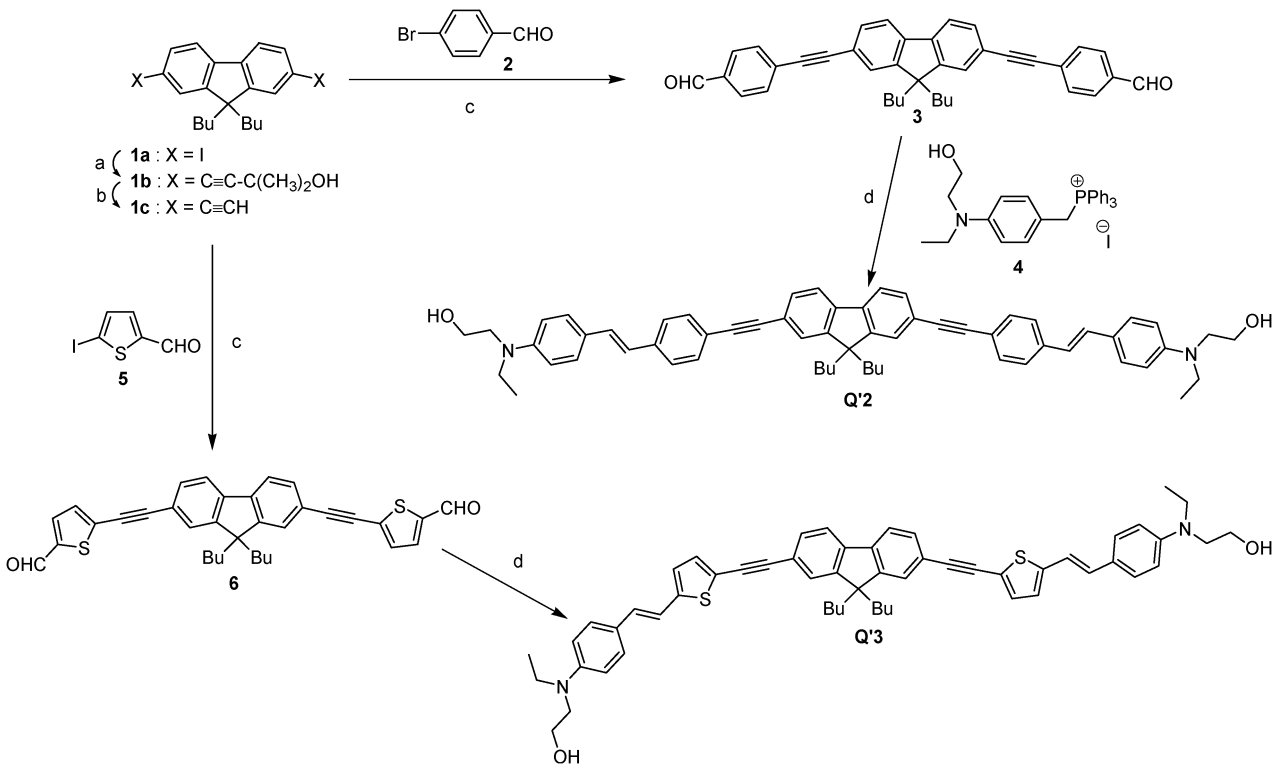

Scheme 1 (a) 2-Methyl-3-butyn-2-ol, $Pd(PPh_3)_2Cl_2$, CuI, toluene/Et_3N, 40 °C, 16 h (87%); (b) KOH, toluene/*i*-PrOH, reflux, 0.5 h (71%); (c) $Pd(PPh_3)_2Cl_2$, CuI, toluene/Et_3N, 40 °C, 16 h (75% for **3** and 97% for **6**); (d) **4**, *t*BuOK, anhyd CH_2Cl_2, 20 °C, 16 h (53% for **Q′2** and 35% for **Q′3**).

Table 1 Photophysical properties of compounds **Q1**, **Q2**, **Q′2** and **Q′3** in toluene

Cpd	λ_{abs}/nm	ε_{max}[a]/M^{-1} cm^{-1}	FWHM/cm^{-1}	f[b]	λ_{em}/nm	Stokes shift/cm^{-1}	Φ_f[c]	τ[d] /ns	k_r[e] (10^9 s^{-1})	k_{nr}[e] (10^9 s^{-1})	τ_0[f] /ns	r[g]	Φ_Δ[h]	Φ_Δ[i]
Q1	387	1.3×10^5	4390	2.3	433	2750	0.82	0.75	1.09	0.24	0.91	0.24	0.05	0.02
Q2	411	1.3×10^5	4730	2.5	464	2780	0.71	0.82	0.87	0.35	1.15	0.23	0.03	0.01
Q′2	406.5	—[j]	4740	—	463.5	3030	0.67	0.79	0.85	0.42	1.18	0.19	0.02	0.01
Q′3	436.5	1.0×10^5	4780	1.9	494.5	2690	0.48	0.93	0.52	0.56	1.94	0.16	0.22	0.12

[a] Molar extinction coefficient. [b] Oscillator strength. [c] Fluorescence quantum yield determined relative to quinine in 0.5 M H_2SO_4. [d] Fluorescence lifetime determined by using time-correlated single-photon counting (TCSPC). [e] Radiative (k_r) and non-radiative (k_{nr}) decay rates. [f] Radiative lifetime. [g] Fluorescence anisotropy. [h] Singlet oxygen formation quantum yield determined relative to tetraphenylporphyrin in toluene (Φ_Δ[TPP] = 0.68 in toluene). [i] Singlet oxygen formation quantum yield determined relative to tetraphenylporphyrin in chloroform (Φ_Δ[TPP] = 0.55 in chloroform). [j] The molar extinction coefficient of **Q′2** has not been measured due to its low solubility in toluene.

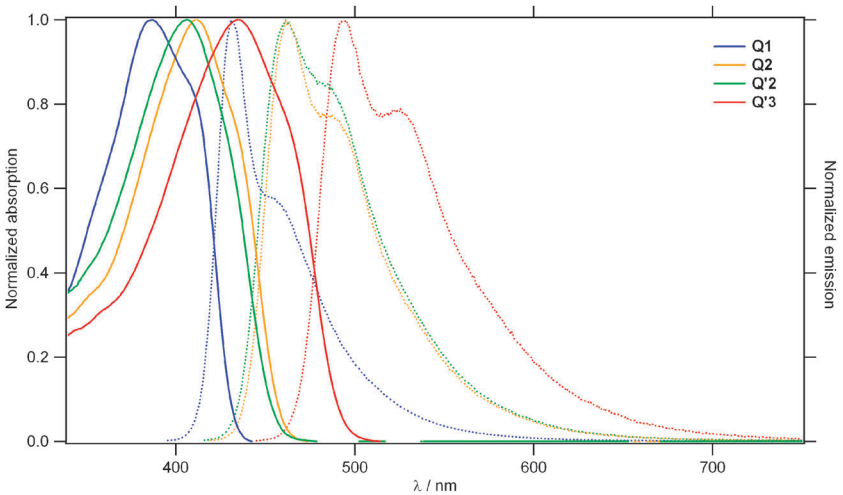

Fig. 1 Normalized absorption and emission spectra of compounds **Q1**, **Q2**, **Q′2** and **Q′3** in toluene.

of the two phenylene units by two thienylene units (**Q′2** → **Q′3**) leads to a marked red-shift of both absorption and emission and induces a significant reduction of the fluorescence quantum yield as a result of combined decrease of the radiative decay rate (in relation with red-shifted emission) and increase of the non-radiative decay rate. This is consistent with a facilitated inter-system crossing ($S_1 \rightarrow T_1$).[58]

Whereas compounds bearing linear alkyl chains **Q1** and **Q2** present a similar fluorescence anisotropy in agreement with a similar size, compound **Q′2** lacking terminal long alkyl chains shows a smaller anisotropy ratio. **Q′3** having similar peripheral (and central) alkyl groups to chromophore **Q′2** reveals a lower anisotropy ratio in agreement with the smaller size of its conjugated system.

Solvatochromism. Table 2 illustrates the dependence of the optical properties of chromophore **Q′3** on solvent polarity and viscosity. All compounds display similar solvatochromic behaviour (see ESI†). Increasing the solvent polarity induces a slight red shift of the absorption band and a marked bathochromic shift of the emission band as clearly illustrated in Fig. 2 for chromophore **Q′3**. This marked positive solvatochromism provides evidence of a highly polar emissive excited-state, in agreement with a localization of the excitation on a dipolar chromophoric subunit in low polarity to high polarity environments.[59]

In low to medium polarity solvents **Q′3** displays significant fluorescence (Φ_f values ranging from 0.5 to 0.6) whereas its fluorescence significantly decreases in high polarity solvents

Table 2 Photophysical properties of compound **Q′3** in different solvents

Solvent	λ_{abs}/nm	λ_{em}/nm	Stokes shift/cm^{-1}	Φ_f[a]	τ/ns	k_r (10^9 s^{-1})	k_{nr} (10^9 s^{-1})	τ_0[b]/ns	r[c]
Toluene	436	493	2650	0.48	0.93	0.52	0.56	1.94	0.16
Bu_2O	433.5	491	2700	0.55	0.99	0.56	0.45	1.79	0.19
$CHCl_3$	431.5	522.5	4035	0.48	1.22	0.39	0.43	2.54	0.15
AcOEt	435	544	4605	0.51	1.42	0.36	0.34	2.77	0.12
DCM	433.5	549.5	4870	0.61	1.43	0.42	0.27	2.35	0.10
THF	437	555	4865	0.51	1.51	0.34	0.32	2.93	0.12
Acetone	437.5	591.5	5950	0.22	0.88	0.25	0.89	4.02	0.13
CH_3CN	436.5	604	6355	0.052	1.03	0.05	0.92	19.99	0.21
DMSO	448.5	617	6090	0.051	0.49	0.10	1.94	9.7	0.28

[a] Fluorescence quantum yield determined relative to quinine in 0.5 M H_2SO_4. [b] Radiative lifetime. [c] Fluorescence anisotropy.

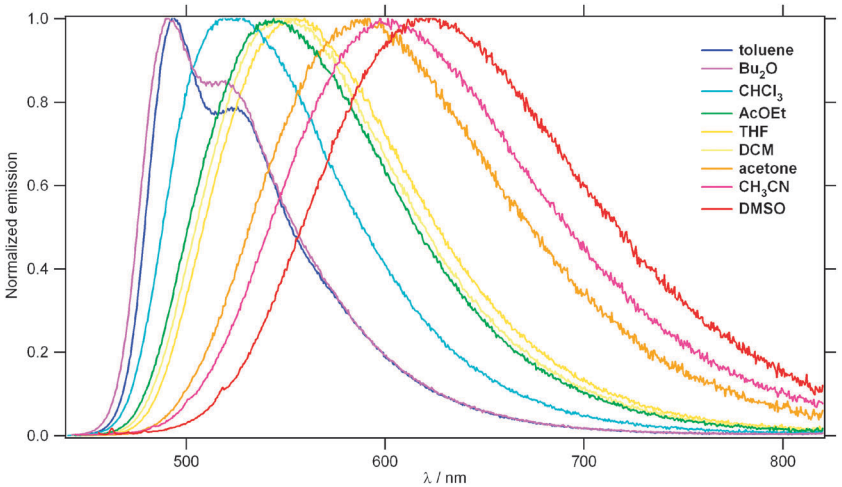

Fig. 2 Normalized emission spectra of fluorophore **Q′3** in solvents of different polarities.

like DMSO, acetone and CH_3CN due to the combination of reduced radiative decay rates (in relation with red-shifted emission) and significant enhancement of the non-radiative decay rates, indicating efficient competing deactivation processes.

As shown in Fig. 3, the solvatochromic behaviour of the quadrupolar chromophores in medium to high polarity solvents can be fitted with a Lippert–Mataga relationship, given in eqn (1).[60,61] The Stokes shift values show a linear dependency on the polarity–polarizability function Δf:

$$\nu_{abs} - \nu_{em} = 2(\Delta\mu^2/hca^3)\Delta f + \text{const} \qquad (1)$$

where ν_{abs} (ν_{em}) is the wavenumber of the absorption (fluorescence) maximum, h is the Planck constant, c is the light velocity, a is the radius of the Onsager cavity, and $\Delta f = (\varepsilon - 1)/(2\varepsilon + 1) - (n^2 - 1)/(2n^2 + 1)$, where ε is the dielectric constant and n the refractive index of the solvent while $\Delta\mu$ is the change of dipole moment of the solute between ground and excited states.

This behaviour is consistent with (medium to high polarity) solvent-induced symmetry breaking occurring in the excited state of quadrupolar chromophores, leading to excitation localization on a dipolar chromophoric subunit (*i.e.* DA portion of the DAD quadrupolar structure).[59] Hence the emission solvatochromism is similar to that of corresponding push–pull chromophores showing strong intramolecular charge transfer transition. The slopes of the corresponding linear regressions (*i.e.* $2\Delta\mu^2/hca^3$) are collected in Table 3. To further derive $\Delta\mu$ values, accurate estimation of the Onsager cavity radius (a) is required. To do so, anisotropy (r) and fluorescence lifetime (τ) measurements have been conducted in solvents of varying viscosity (η) in order to determine the molecular size of the quadrupolar chromophores.

Using the Perrin equation (eqn (2)),[62] one can derive—from the linear variation of $(0.4/r - 1)$ as a function of τ/η (see Fig. 4)—the effective molecular volume (v) and subsequently estimate the Onsager cavity radius a (estimated as one-half of the quadrupolar molecule radius in relation with excitation localization on a dipolar chromophoric subunit).

$$r_{max} = \frac{0.4}{1 + \frac{\tau kT}{\eta v}} \qquad (2)$$

Table 3 Molecular sizes (long axis R) and excited-state dipole moments of chromophores **Q1**, **Q2**, **Q′2** and **Q′3** derived from fluorescence solvatochromism and anisotropy studies

Compound	R^a/Å	a^b/Å	Lippert–Mataga slope^c (10^3 cm^{-1})	$\Delta\mu$/D
Q1	13.1	6.55	24.6	27
Q2	12.9	6.45	19.6	23
Q′2	11.6	5.8	19.1	20
Q′3	11.1	5.55	17.1	17

[a] Molecular radius derived from fluorescence anisotropy. [b] Dipolar Onsager cavity radius. [c] Slope derived from the linear dependence of the Stokes shift on the solvent polarity–polarizability function Δf.

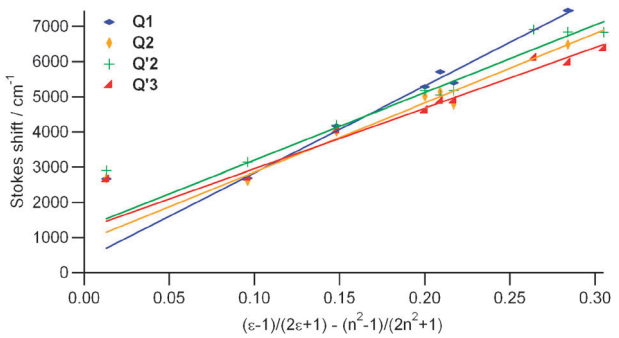

Fig. 3 Lippert–Mataga correlations for chromophores **Q1**, **Q2**, **Q′2** and **Q′3**.

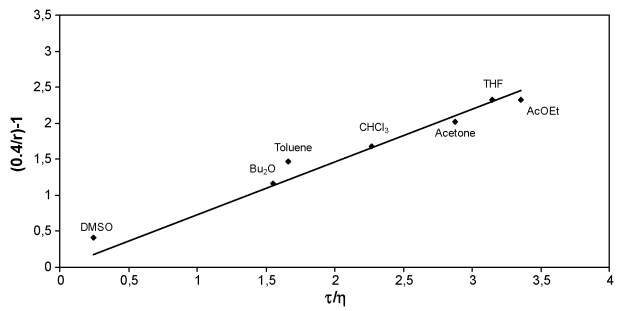

Fig. 4 Perrin plot from the variation of the fluorescence anisotropy of **Q′3** in a series of solvents of different viscosities.

The data are collected in Table 3. As expected quadrupolar chromophores **Q1**/**Q2** (bearing long alkyl chains) exhibit larger molecular radius than chromophores that only have short alkyl chains on the end-groups (**Q′2**/**Q′3**). In contrast quadrupolar chromophore **Q′3** has a smaller radius due its shorter and less rigid conjugated system. We observe that chromophore **Q1** having the more rigid extended system leads to the largest $\Delta\mu$ value (27 D) whereas the shortest chromophore **Q′3** shows the smallest one (17 D). We also note that the presence of the hydroxyethyl chain on **Q′2** leads to a slightly smaller excited-state dipole than for **Q2**, indicating that the presence of the alcohol moiety influences the intramolecular charge transfer transition.

Photosensitizing ability: singlet oxygen generation. The $^1O_2$ luminescence at 1272 nm of the four samples (**Q1**, **Q2**, **Q′2** and **Q′3**) was measured both in toluene and in chloroform by comparison with a tetraphenylporphyrin reference solution measured in the same solvents. The singlet oxygen quantum yield (Φ_Δ) values are gathered in Table 1. For each compound, we observe an increase of the singlet oxygen quantum yield from chloroform to toluene and for both solvents the highest values of Φ_Δ obtained are for the quadrupole **Q′3**. Furthermore the same trend is observed whatever the solvent used. The first three chromophores present an important fluorescence emission which induces very low singlet oxygen quantum yields (Φ_Δ). In contrast, the less aromatic thienyl fluorescent compound **Q′3** favours a non-negligible generation of singlet oxygen as well as a reasonable fluorescence emission as was initially required for allowing both targeting monitoring (by fluorescence imaging) and therapy (by photosensitized production of singlet oxygen). It should be noticed that the largest singlet oxygen quantum yield is correlated with the smallest dipole moment of the emissive excited state, in agreement with the fact that an increase of intramolecular charge transfer usually competes with processes leading to singlet oxygen production (*i.e.* intersystem crossing and energy transfer to oxygen).[63,64]

Based on the experimental results, to further increase the singlet oxygen quantum yield (but at the expense of a decrease of the residual fluorescence), a possible way for the optimization of these systems could be the introduction of additional thienylene units in the conjugated system. This would most probably lead to an improved singlet oxygen/fluorescence ratio for application in PDT.

Two-photon absorption (TPA). The TPA spectra of the fluorophores were determined in the NIR range (700–980 nm) by investigating their two-photon excited fluorescence (TPEF) in solution. The measurements were performed under excitation with 150 fs pulses from a Ti:sapphire laser by using the experimental protocol of Xu and Webb.[65] Table 4 and Fig. 5 show, respectively, TPA cross-section values and spectra of the compounds **Q1**, **Q2**, **Q′2** and **Q′3** in THF (which is a relevant model of the polarity that such lipophilic chromophores could experiment when wrapped within dendrimeric sheaths).[39]

For all compounds, we observe intense and broad TPA bands in the NIR region. For strictly centrosymmetrical quadrupoles, the one-photon excited state is expected to have no or little TPA activity and the lower energy two-photon-allowed excited state to lie at higher energy. However, due to the banana-shape of the investigated series of compounds, we observe in all cases a TPA band (or shoulder in the case of chromophore **Q′3**) which lies at about twice the one-photon (OPA) maximum absorption wavelength. The higher lying maximum (as well as an additional higher lying strongly allowed maximum) is observed only in the case of chromophore **Q′3**. We notice that all chromophores present broad absorption bands with a shoulder extending to an even lower energy than the one photon-allowed excited state. This is indicative of strong electron–phonon coupling.

As illustrated in Fig. 5 and already reported for analogous rod-like chromophores,[35] the substitution of a triple bond (**Q1**) by a double bond (**Q2**) leads to a large increase of the TPA cross-section values in the NIR region (with a significant broadening and red-shift of the TPA spectrum). Indeed, the fluorophores built from vinylene linkers (**Q2**, **Q′2** and **Q′3**) instead of ethynylene linkers (**Q1**) reveal much larger TPA cross-section values in the whole NIR region, this effect being

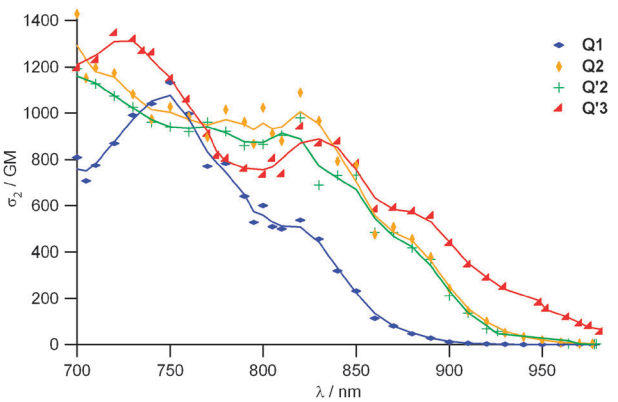

Fig. 5 TPA spectra of **Q1**, **Q2**, **Q′2** and **Q′3** in THF (with solid curves as guides for the eyes only).

Table 4 Two-photon absorption data of compounds **Q1**, **Q2**, **Q′2** and **Q′3** in THF

					$\sigma_2{}^a$/GM		
Cpd	$2\lambda_{max}{}^{OPA}$/nm	$\lambda_{max1}{}^{TPA}$/nm	$\lambda_{max2}{}^{TPA}$/nm	$\lambda_{max3}{}^{TPA}$/nm	At $\lambda_{max1}{}^{TPA}$	At $\lambda_{max2}{}^{TPA}$	At $\lambda_{max3}{}^{TPA}$
Q1	774	750	<700	—	1130	—	—
Q2	824	820	≤ 700	—	1090	≥ 1430	—
Q′2	822	820	≤ 700	—	980	≥ 1190	—
Q′3	874	870	820	730	600	940	1340

[a] 1 GM = 10^{-50} cm^4 s photon^{-1}; TPA measurements were performed using a mode-locked Ti:sapphire laser delivering 150 fs pulses at a repetition rate of 76 MHz, using fluorescein as a reference.

more pronounced in the longer wavelength range. More strikingly, chromophore **Q′2** seems to show slightly lower TPA responses than chromophore **Q2** (however close to the limit of the experimental errors), which could indicate that the slightly different environment provided by the presence of only two alcohol moieties—although non-conjugated—in close proximity to the chromophoric unit affects the charge redistribution (as was suggested by the slightly lower excited-state dipole) occurring upon excitation and also the TPA responses.

Finally chromophore **Q′3** owns both the largest TPA responses and the broader spectrum in the spectral range of interest for biomedical applications (three different maxima are observed in the 750–950 nm range). This result can be related to the introduction of low-aromaticity thiophene heterocycles in the conjugated system, in agreement with the essential-state model[52,53] and previously reported experimental results.[35]

Hence this chromophore meets all the prerequisites for its use as a biphotonic sensitizer for PDT by two-photon excitation in the spectral range of interest for biomedical applications while allowing 3D mapping by two-photon excited fluorescence imaging. In addition, the presence of two alcohol end-groups provides an easy way for further functionalization by covalent grafting on various platforms and/or covalent attachment of targeting moieties.

Conclusion

Symmetrical banana-shaped bis-donor fluorophores were prepared from the symmetrical functionalization of a fluorenyl core bearing elongated conjugated rods made from arylene–vinylene or arylene–ethynylene building blocks in order to test modifications which could increase singlet oxygen production ability while maintaining some fluorescence and large TPA responses. As was anticipated, the replacement of phenylene moieties by less aromatic thienylene moieties in the conjugated rods gave rise to both enhancement and broadening of the TPA responses in the spectral region of interest for biomedical applications. Moreover, this replacement also led to a major increase of the singlet oxygen production ability (by a factor of ten compared to a structural analogue) while keeping residual fluorescence, in relation with the increase of the intersystem crossing. The experimental study also gives some trends for further tentative improvement of the biphotonic sensitizer. This could possibly be achieved by increasing the number of thienyl units in the conjugated linker (also leading to red-shift of the TPA spectrum), keeping in mind that combination with phenyl units seems also needed not to decrease the TPA responses[35] and maintain a suitable triplet excited state energy level. Hence a subtle compromise has to be achieved to improve both singlet oxygen production and TPA.

The molecular optimization study shows that chromophore **Q′3**—which combines large TPA responses in the whole spectral range of interest, reasonable singlet oxygen production ability and residual fluorescence—offers promises for highly selective spatially-resolved two-photon PDT, based on the combination of such a graftable sensitizer with targeting units that could allow sensitive detection (3D mapping by two photon-excited fluorescence) of tumour cells. In particular encapsulation of biphotonic fluorophores[66–69] or biphotonic sensitizers[15,70,71] within nanoparticles has been shown to be of high interest for preserving photophysical properties in aqueous media (including singlet oxygen production) and to yield nano-object with very high TPA. In addition the nanoparticle approach offers high flexibility for combination of chromophores and targeting units within single nano-objects.[48,51] We are currently implementing such a modular strategy.

Experimental section

Synthetic procedures

General methods. All air- or water-sensitive reactions were carried out under dry argon. Solvents were generally dried and distilled prior to use. Reactions were monitored by thin-layer chromatography on Merck silica gel 60 F_{254} precoated aluminium sheets. Column chromatography: Merck silica gel Si 60 (40–63 μm, 230–400 mesh or 63–200 μm, 70–230 mesh). Melting points were determined on an Electrothermal IA9300 digital melting point instrument. NMR: Bruker ARX 200 (^{1}H: 200.13 MHz, ^{13}C: 50.32 MHz) or Avance AV 300 (^{1}H: 300.13 MHz, ^{13}C: 75.48 MHz), in $CDCl_3$ solutions; ^{1}H chemical shifts (δ) are given in ppm relative to TMS as internal standard, J values in Hz and ^{13}C chemical shifts relative to the central peak of $CDCl_3$ at 77.0 ppm. High and low resolution mass spectra measurements were performed at the Centre Régional de Mesures Physiques de l'Ouest (C.R.M.P.O., Rennes), using a Micromass MS/MS ZABSpec TOF instrument with EBE TOF geometry; LSIMS (Liquid Secondary Ion Mass Spectrometry) at 8 kV with Cs^+ in *m*-nitrobenzyl alcohol (mNBA); ES+ (electrospray ionization, positive mode) at 4 kV; EI (electron ionization) at 70 eV. Elemental analyses were performed at C.R.M.P.O. Compounds **Q1**,[35] **Q2**,[35] **1a**,[55] **4**[57] and **5**[56] were synthesized according to the respective literature procedures.

4,4′-(9,9-Dibutyl-9*H*-fluorene-2,7-diyl)bis(2-methyl-3-butyn-2-ol) (1b). Air was removed from a solution of **1a**[55] (6.00 g, 11.3 mmol) in 37.5 mL of toluene/Et_3N (5/1) by blowing argon for 20 min. Then CuI (86 mg, 0.45 mmol), $Pd(PPh_3)_2Cl_2$ (316 mg, 0.45 mmol) and 2-methyl-3-butyn-2-ol (2.84 g, 33.8 mmol) were added, and the mixture was stirred at 40 °C for 16 h. After evaporation of the solvent, the residue was purified by column chromatography (heptane/CH_2Cl_2 30 : 70 then CH_2Cl_2) to yield 4.37 g (87%) of 4,4′-(9,9-dibutyl-9*H*-fluorene-2,7-diyl)bis(2-methyl-3-butyn-2-ol) (**1b**): ^{1}H NMR (200.13 MHz, $CDCl_3$) δ 7.60 (d, J = 8.6 Hz, 2H), 7.40 (d, J = 8.6 Hz, 2H), 7.38 (s, 2H), 2.16 (s, 2H), 1.94 (m, 4H), 1.66 (s, 12H), 1.07 (m, 4H), 0.66 (t, J = 7.3, 6H), 0.52 (m, 4H); ^{13}C NMR (50.32 MHz, $CDCl_3$) δ 150.8, 140.5, 130.7, 126.0, 121.3, 119.8, 93.9, 82.9, 65.7, 55.0, 40.1, 31.5, 25.7, 23.0, 13.8; HRMS (EI) calcd for $C_{31}H_{38}O_2$ ($M^{+\bullet}$) m/z 442.2872, found 442.2859. Anal. calcd for $C_{31}H_{38}O_2$ (442.64): C, 84.12; H, 8.65. Found: C, 84.01; H, 8.71%.

2,7-Diethynyl-9,9-dibutyl-9*H*-fluorene (1c). To a solution of **1b** (1.04 g, 2.35 mmol) in 20 mL of toluene/*i*-PrOH (3/1) was added solid KOH (0.39 g). The mixture was heated under reflux for 0.5 h. After cooling, KOH was filtered off and the solvents were evaporated and the residue was purified

by column chromatography (heptane/CH_2Cl_2 70 : 30 then 20 : 80) to yield 0.54 g (71%) of **1c**: ^{1}H NMR (200.13 MHz, $CDCl_3$) δ 7.63 (d, J = 8.6 Hz, 2H), 7.48 (d, J = 8.6 Hz, 2H), 7.46 (s, 2H), 3.15 (s, 2H), 1.94 (m, 4H), 1.07 (m, 4H), 0.67 (t, J = 7.2 Hz, 6H), 0.54 (m, 4H); ^{13}C NMR (50.32 MHz, $CDCl_3$) δ 151.0, 140.9, 131.2, 126.5, 120.8, 119.9, 84.5, 77.4, 55.1, 40.0, 25.8, 22.9, 13.7; HRMS (EI) calcd for $C_{25}H_{26}$ ($M^{+\bullet}$) m/z 326.2035, found 326.2036. Anal. calcd for $C_{25}H_{26}$ (326.48): C, 91.97; H, 8.03. Found: C, 92.17; H, 8.07%.

4,4′-(9,9-Dibutyl-9*H*-fluorene-2,7-diyldi-2,1-ethynediyl)bis-benzaldehyde (3). Air was removed from a solution of **1c** (0.251 g, 0.766 mmol) and **2** (0.354 g, 1.914 mmol) in 10 mL of toluene/Et_3N (4/1) by blowing argon for 20 min. Then CuI (6.0 mg, 0.031 mmol) and $Pd(PPh_3)_2Cl_2$ (22 mg, 0.031 mmol) were added, and deaeration was continued for 10 min. Thereafter the mixture was stirred at 40 °C for 16 h. The solvent was removed under reduced pressure, and the crude product was purified by column chromatography (heptane/CH_2Cl_2 50 : 50 then 40 : 60) to yield 307 mg (75%) of **3**; ^{1}H NMR (300.13 MHz, $CDCl_3$) δ 9.94 (s, 2H), 7.80 (d, J = 8.4 Hz, 4H), 7.63 (d, J = 8.4 Hz, 4H), 7.62 (d, J = 8.7 Hz, 2H), 7.48 (d, J = 8.7 Hz, 2H), 7.46 (s, 2H), 1.94 (m, 4H), 1.05 (m, 4H), 0.60 (t, J = 7.2 Hz, 6H), 0.53 (m, 4H); ^{13}C NMR (75.46 MHz, $CDCl_3$) δ 191.3, 151.2, 141.1, 135.4, 132.0, 131.1, 129.6, 126.2, 121.4, 120.3, 94.5, 89.2, 55.3, 40.2, 25.9, 22.9, 13.8; HRMS (ESI) calcd for $C_{39}H_{35}O_2$ [$(M + H)^+$] m/z 535.26371, found 535.2638.

5,5′-(9,9-Dibutyl-9*H*-fluorene-2,7-diyldi-2,1-ethynediyl)bis-2-thiophenecarboxaldehyde (6). Air was removed from a solution of **1c** (0.150 g, 0.460 mmol) and **5**[56] (0.251 g, 1.06 mmol) in 6.5 mL of toluene/Et_3N (4/1) by blowing argon for 20 min. Then CuI (7.0 mg, 0.037 mmol) and $Pd(PPh_3)_2Cl_2$ (27 mg, 0.039 mmol) were added, and deaeration was continued for 10 min. Thereafter the mixture was stirred at 40 °C for 16 h. The solvent was removed under reduced pressure, and the crude product was purified by column chromatography (heptane/CH_2Cl_2 50 : 50 then 40 : 60) to yield 245 mg (97%) of **6**; ^{1}H NMR (300.13 MHz, $CDCl_3$) δ 9.80 (s, 2H), 7.61 and 7.26 (AX, J_{AX} = 3.9 Hz, 4H), 7.62 (d, J = 8.5 Hz, 2H), 7.47 (d, J = 8.5 Hz, 2H), 7.45 (s, 2H), 1.93 (m, 4H), 1.02 (m, 4H), 0.60 (t, J = 7.3 Hz, 6H), 0.51 (m, 4H); ^{13}C NMR (75.46 MHz, $CDCl_3$) δ 182.4, 151.4, 143.9, 141.4, 136.1, 133.0, 132.5, 131.0, 126.0, 120.9, 120.4, 98.9, 82.6, 55.3, 40.1, 25.9, 23.0, 13.8; HRMS (ESI) calcd for $C_{35}H_{30}O_2S_2$ ($M^{+\bullet}$) m/z 546.16872, found 546.1687.

Fluorophore Q′2. To a solution of **3** (0.100 g, 0.187 mmol) and **4**[57] (0.244 g, 0.430 mmol) in anhydrous CH_2Cl_2 (4 mL) was added *t*BuOK (0.063 g, 0.561 mmol). The mixture was stirred at 20 °C for 16 h, then filtered through a short pad of silica gel. The solvent was removed under reduced pressure, and the crude product was purified by column chromatography (CH_2Cl_2/AcOEt 98 : 2 then 95 : 5) to yield 85 mg (53%) of **Q′2**; ^{1}H NMR (200.13 MHz, $CDCl_3$) δ 7.67 (d, J = 7.7 Hz, 2H), 7.53 (d, J = 7.7 Hz, 2H), 7.52 (m, 2H), 7.53 and 7.47 (AA′BB′, J_{AB} = 8.5 Hz, 8H), 7.41 and 6.76 (AA′XX′, J_{AX} = 8.7 Hz, 8H), 7.08 (d, J = 16.1 Hz, 2H), 6.90 (d, J = 16.1 Hz, 2H), 3.83 (t, J = 5.5 Hz, 4H), 3.51 (t, J = 5.5 Hz, 4H), 3.47 (q, J = 7.0 Hz, 4H), 1.99 (m, 4H), 1.19 (t, J = 7.0 Hz, 6H), 1.07 (m, 4H), 0.69 (t, J = 7.3 Hz, 6H), 0.60 (m, 4H); HRMS (ESI) calcd for $C_{61}H_{65}N_2O_2$ [$(M + H)^+$] m/z 857.5046, found 857.5046. Anal. calcd for $C_{61}H_{64}N_2O_2$ (857.19): C, 85.47; H, 7.53; N, 3.27. Found: C, 85.01; H, 7.71; N, 3.32%.

Fluorophore Q′3. To a solution of **6** (0.241 g, 0.441 mmol) and **4**[57] (0.576 g, 1.016 mmol) in anhydrous CH_2Cl_2 (10 mL) was added *t*BuOK (0.149 g, 1.325 mmol). The mixture was stirred at 20 °C for 16 h, then filtered through a short pad of silica gel. The solvent was removed under reduced pressure, and the crude product was purified by column chromatography (CH_2Cl_2/AcOEt 98 : 2 then 95 : 5) to yield 134 mg (35%) of **Q′3**; ^{1}H NMR (300.13 MHz, $CDCl_3$) δ 7.66 (d, J = 8.0 Hz, 2H), 7.50 (d, J = 8.0 Hz, 2H), 7.48 (m, 2H), 7.35 and 6.73 (AA′XX′, J_{AX} = 8.9 Hz, 8H), 7.17 and 6.89 (AX, J_{AX} = 3.6 Hz, 4H), 6.98 (d, J = 16.0 Hz, 2H), 6.85 (d, J = 16.0 Hz, 2H), 3.81 (t, J = 5.7 Hz, 4H), 3.50 (t, J = 5.7 Hz, 4H), 3.50 (q, J = 7.1 Hz, 4H), 1.99 (m, 4H), 1.66 (s, 2H), 1.18 (t, J = 7.0 Hz, 6H), 1.07 (m, 4H), 0.69 (t, J = 7.3 Hz, 6H), 0.59 (m, 4H); ^{13}C NMR (75.46 MHz, $CDCl_3$) δ 151.1, 148.1, 145.8, 140.7, 132.7, 130.5, 129.6, 127.9, 125.6, 125.0, 124.8, 121.8, 120.4, 120.0, 117.2, 112.5, 94.9, 84.0, 60.3, 55.2, 52.4, 45.6, 40.2, 25.9, 23.1, 13.9, 12.0; HRMS (ESI) calcd for $C_{57}H_{61}N_2O_2S_2$ [$(M + H)^+$] m/z 869.41745, found 869.4173.

Photophysical methods

All photophysical properties measurements have been performed with freshly-prepared air-equilibrated solutions at room temperature (298 K). UV/Vis absorption spectra were recorded on a Jasco V-570 spectrophotometer. Steady-state and time-resolved fluorescence measurements were performed on dilute solutions (*ca.* 10^{-6} M, optical density < 0.1) contained in standard 1 cm quartz cuvettes using an Edinburgh Instruments (FLS920) spectrometer in photon-counting mode. Fully corrected emission spectra were obtained, for each compound, at $\lambda_{ex} = \lambda_{max}^{abs}$ with an optical density at $\lambda_{ex} \leq 0.1$ to minimize internal absorption. Fluorescence quantum yields were measured according to literature procedures.[72,73] Fluorescence lifetimes were measured by time correlated single-photon counting (TCSPC) by using the same FLS 920 fluorimeter. Excitation was achieved by a hydrogen-filled nanosecond flashlamp (repetition rate 40 kHz). The instrument response (FWHM *ca.* 1 ns) was determined by measuring the light scattered by a Ludox suspension. The TCSPC traces were analyzed by standard iterative reconvolution methods implemented in the software of the fluorimeter. All compounds displayed strictly mono-exponential fluorescence decays ($\chi^2 < 1.1$).

Two-photon absorption

Two-photon absorption (TPA) measurements were conducted by investigating the two-photon excited fluorescence (TPEF) of the fluorophores in THF at room temperature on air-equilibrated solutions (10^{-4} M), according to the experimental protocol established by Xu and Webb.[65] This protocol avoids contributions from excited-state absorption that are known to result in largely overestimated TPA cross-sections. To span the 700–980 nm range, a Nd:YLF-pumped Ti:sapphire oscillator

was used generating 150 fs pulses at a 76 MHz rate. The excitation was focused into the cuvette through a microscope objective (10×, NA 0.25). The fluorescence was detected in epifluorescence mode *via* a dichroic mirror (Chroma 675dcxru) and a barrier filter (Chroma e650sp-2p) by a compact CCD spectrometer module BWTek BTC112E. Total fluorescence intensities were obtained by integrating the corrected emission spectra measured by this spectrometer. TPA cross-sections (σ_2) were determined from the two-photon excited fluorescence (TPEF) cross-sections ($\sigma_2\Phi_f$) and the fluorescence emission quantum yield (Φ_f). TPEF cross-sections were measured relative to fluorescein in 0.01 M aqueous NaOH for 715–980 nm,[65,74] and the appropriate solvent-related refractive index corrections.[75] Data points between 700 and 715 nm were corrected according to ref. 76. The quadratic dependence of the fluorescence intensity on the excitation power was checked for each sample and all wavelengths, indicating that the measurements were carried out in intensity regimes where saturation or photodegradation did not occur.

Measurements of singlet oxygen quantum yield (Φ_Δ)

The excitation source consisted of a Xe-arc, the light was separated in a SPEX 1680, 0.22 μm double monochromator. The detection at 1270 nm was done through a PTI S/N 1565 monochromator, and the emission was monitored by a liquid nitrogen-cooled Ge-detector model (EO-817L, North Coast Scientific Co). Singlet oxygen quantum yields Φ_Δ were determined using tetraphenylporphyrin (TPP) as reference solution (Φ_Δ [TPP] = 0.55 in $CHCl_3$[77]; Φ_Δ [TPP] = 0.68 in toluene)[44] and were estimated from $^1O_2$ luminescence at 1272 nm. The optical density of the reference and the sample solution (at 405 nm) were set equal to 0.2.

Acknowledgements

Financial support by ANR PNANO 07-102 is gratefully acknowledged. We thank Région Bretagne for a fellowship to CR. Part of the work was supported by GDR Photomed.

References and notes

1 G. S. He, L.-S. Tan, Q. Zheng and P. N. Prasad, *Chem. Rev.*, 2008, **108**, 1245–1330.
2 F. Terenziani, C. Katan, E. Badaeva, S. Tretiak and M. Blanchard-Desce, *Adv. Mater.*, 2008, **20**, 4641–4678.
3 M. Pawlicki, H. A. Collins, R. G. Denning and H. L. Anderson, *Angew. Chem., Int. Ed.*, 2009, **48**, 3244–3266.
4 H. M. Kim and B. R. Cho, *Chem. Commun.*, 2009, 153–164.
5 S. Maruo, O. Nakamura and S. Kawata, *Opt. Lett.*, 1997, **22**, 132–134.
6 B. H. Cumpston, S. P. Ananthavel, S. Barlow, D. L. Dyer, J. E. Ehrlich, L. L. Erskine, A. A. Heikal, S. M. Kuebler, I.-Y. S. Lee, D. McCord-Maughon, J. Qin, H. Röckel, M. Rumi, X. L. Wu, S. R. Marder and J. W. Perry, *Nature*, 1999, **398**, 51–54.
7 S. Kawata, H.-B. Sun, T. Tanaka and K. Takada, *Nature*, 2001, **412**, 697–698.
8 D. A. Parthenopoulos and P. M. Rentzepis, *Science*, 1989, **245**, 843–845.
9 J. H. Strickler and W. W. Webb, *Opt. Lett.*, 1991, **16**, 1780–1782.
10 G. S. He, G. C. Xu, P. N. Prasad, B. A. Reinhardt, J. C. Bhatt, R. McKellar and A. G. Dillard, *Opt. Lett.*, 1995, **20**, 435–437.
11 J. E. Ehrlich, X. L. Wu, I. Y. S. Lee, Z. Y. Hu, H. Röckel, S. R. Marder and J. W. Perry, *Opt. Lett.*, 1997, **22**, 1843–1845.
12 W. Denk, J. H. Strickler and W. W. Webb, *Science*, 1990, **248**, 73–76.
13 C. Xu, W. Zipfel, J. B. Shear, R. M. Williams and W. W. Webb, *Proc. Natl. Acad. Sci. U. S. A.*, 1996, **93**, 10763–10768.
14 J. D. Bhawalkar, N. D. Kumar, C. F. Zhao and P. N. Prasad, *J. Clin. Laser Med. Surg.*, 1997, **15**, 201–204.
15 S. Kim, T. Y. Ohulchanskyy, H. E. Pudavar, R. K. Pandey and P. N. Prasad, *J. Am. Chem. Soc.*, 2007, **129**, 2669–2675.
16 H. A. Collins, M. Khurana, E. H. Moriyama, A. Mariampillai, E. Dahlstedt, M. Balaz, M. K. Kuimova, M. Drobizhev, X. D. YangVictor, D. Phillips, A. Rebane, B. C. Wilson and H. L. Anderson, *Nat. Photonics*, 2008, **2**, 420.
17 J. R. Starkey, A. K. Rebane, M. A. Drobizhev, F. Meng, A. Gong, A. Elliott, K. McInnerney and C. W. Spangler, *Clin. Cancer Res.*, 2008, **14**, 6564–6573.
18 H. M. Kim and B. R. Cho, *Acc. Chem. Res.*, 2009, **42**, 863–872.
19 H. M. Kim and B. R. Cho, *Chem.–Asian J.*, 2011, **6**, 58–69.
20 S. Sumalekshmy and C. J. Fahrni, *Chem. Mater.*, 2010, **23**, 483–500.
21 P. R. Ogilby, *Chem. Soc. Rev.*, 2010, **39**, 3181–3209, and references cited therein.
22 M. Drobizhev, A. Karotki, M. Kruk and A. Rebane, *Chem. Phys. Lett.*, 2002, **355**, 175–182.
23 H. Rath, J. Sankar, V. PrabhuRaja, T. K. Chandrashekar, A. Nag and D. Goswami, *J. Am. Chem. Soc.*, 2005, **127**, 11608–11609.
24 R. Misra, R. Kumar, T. K. Chandrashekar, A. Nag and D. Goswami, *Org. Lett.*, 2006, **8**, 629–631.
25 K. Ogawa, A. Ohashi, Y. Kobuke, K. Kamada and K. Ohta, *J. Am. Chem. Soc.*, 2003, **125**, 13356–13357.
26 D. Y. Kim, T. K. Ahn, J. H. Kwon, D. Kim, T. Ikeue, N. Aratani, A. Osuka, M. Shigeiwa and S. Maeda, *J. Phys. Chem. A*, 2005, **109**, 2996–2999.
27 T. K. Ahn, K. S. Kim, D. Y. Kim, S. B. Noh, N. Aratani, C. Ikeda, A. Osuka and D. Kim, *J. Am. Chem. Soc.*, 2006, **128**, 1700–1704.
28 K. Ogawa, H. Hasegawa, Y. Inaba, Y. Kobuke, H. Inouye, Y. Kanemitsu, E. Kohno, T. Hirano, S.-i. Ogura and I. Okura, *J. Med. Chem.*, 2006, **49**, 2276–2283.
29 L. Ventelon, L. Moreaux, J. Mertz and M. Blanchard-Desce, *Chem. Commun.*, 1999, 2055–2056.
30 L. Ventelon, S. Charier, L. Moreaux, J. Mertz and M. Blanchard-Desce, *Angew. Chem., Int. Ed.*, 2001, **40**, 2098–2101.
31 O. Mongin, L. Porrès, L. Moreaux, J. Mertz and M. Blanchard-Desce, *Org. Lett.*, 2002, **4**, 719–722.
32 M. G. Silly, L. Porrès, O. Mongin, P.-A. Chollet and M. Blanchard-Desce, *Chem. Phys. Lett.*, 2003, **379**, 74–80.
33 M. H. V. Werts, S. Gmouh, O. Mongin, T. Pons and M. Blanchard-Desce, *J. Am. Chem. Soc.*, 2004, **126**, 16294–16295.
34 M. Charlot, N. Izard, O. Mongin, D. Riehl and M. Blanchard-Desce, *Chem. Phys. Lett.*, 2006, **417**, 297–302.
35 O. Mongin, L. Porrès, M. Charlot, C. Katan and M. Blanchard-Desce, *Chem.–Eur. J.*, 2007, **13**, 1481–1498.
36 M. Blanchard-Desce, *C. R. Phys.*, 2002, **3**, 439–448.
37 O. Mongin, T. R. Krishna, M. H. V. Werts, A.-M. Caminade, J.-P. Majoral and M. Blanchard-Desce, *Chem. Commun.*, 2006, 915–917.
38 T. R. Krishna, M. Parent, M. H. V. Werts, L. Moreaux, S. Gmouh, S. Charpak, A.-M. Caminade, J.-P. Majoral and M. Blanchard-Desce, *Angew. Chem., Int. Ed.*, 2006, **45**, 4645–4648.
39 O. Mongin, A. Pla-Quintana, F. Terenziani, D. Drouin, C. Le Droumaguet, A.-M. Caminade, J.-P. Majoral and M. Blanchard-Desce, *New J. Chem.*, 2007, **31**, 1354–1367.
40 P. K. Frederiksen, M. Jørgensen and P. R. Ogilby, *J. Am. Chem. Soc.*, 2001, **123**, 1215–1221.
41 S. P. McIlroy, E. Clo, L. Nikolajsen, P. K. Frederiksen, C. B. Nielsen, K. V. Mikkelsen, K. V. Gothelf and P. R. Ogilby, *J. Org. Chem.*, 2005, **70**, 1134–1146.
42 C. B. Nielsen, M. Johnsen, J. Arnbjerg, M. Pittelkow, S. P. McIlroy, P. R. Ogilby and M. Jorgensen, *J. Org. Chem.*, 2005, **70**, 7065–7079.
43 R. Shukla, T. P. Thomas, J. Peters, A. Kotlyar, A. Myc and J. J. R. Baker, *Chem. Commun.*, 2005, 5739–5741.
44 M. Boisbrun, R. Vanderesse, P. Engrand, A. Olié, S. Hupont, J.-B. Regnouf-de-Vains and C. Frochot, *Tetrahedron*, 2008, **64**, 3494–3504.

45 N. Thomas, D. Bechet, P. Becuwe, L. Tirand, R. Vanderesse, C. Frochot, F. Guillemin and M. Barberi-Heyob, *J. Photochem. Photobiol., B*, 2009, **96**, 101–108.
46 S. Hong, P. R. Leroueil, I. J. Majoros, B. G. Orr, J. R. Baker and M. M. Banaszak Holl, *Chem. Biol.*, 2007, **14**, 107–115.
47 J. Gravier, R. Schneider, C. Frochot, T. Bastogne, F. Schmitt, J. Didelon, F. Guillemin and M. Barberi-Heyob, *J. Med. Chem.*, 2008, **51**, 3867–3877.
48 D. Brevet, M. Gary-Bobo, L. Raehm, S. Richeter, O. Hocine, K. Amro, B. Loock, P. Couleaud, C. Frochot, A. Morere, P. Maillard, M. Garcia and J.-O. Durand, *Chem. Commun.*, 2009, 1475–1477.
49 O. Mongin, C. Rouxel, A.-C. Robin, A. Pla-Quintana, T. R. Krishna, G. Recher, F. Tiaho, A.-M. Caminade, J.-P. Majoral and M. Blanchard-Desce, *Proc. SPIE–Int. Soc. Opt. Eng.*, 2008, **7040**, 704006.
50 H. Y. Woo, B. Liu, B. Kohler, D. Korystov, A. Mikhailovsky and G. C. Bazan, *J. Am. Chem. Soc.*, 2005, **127**, 14721–14729.
51 Y.-E. L. Koo, G. R. Reddy, M. Bhojani, R. Schneider, M. A. Philbert, A. Rehemtulla, B. D. Ross and R. Kopelman, *Adv. Drug Delivery Rev.*, 2006, **58**, 1556–1577.
52 M. Barzoukas and M. Blanchard-Desce, *J. Chem. Phys.*, 2000, **113**, 3951–3959.
53 M. Barzoukas and M. Blanchard-Desce, *Nonlinear Opt.*, 2001, **27**, 209–218.
54 B. Kraabel, D. Moses and A. J. Heeger, *J. Chem. Phys.*, 1995, **103**, 5102–5108.
55 F. Li, Z. Chen, W. Wei, H. Cao, Q. Gong, F. Teng, L. Qian and Y. Wang, *J. Phys. D: Appl. Phys.*, 2004, **37**, 1613–1616.
56 L.-H. Wu, C.-S. Chu, N. Janarthanan and C.-S. Hsu, *J. Polym. Res.*, 2000, **7**, 125–134.
57 L. Porrès, B. K. G. Bhatthula and M. Blanchard-Desce, *Synthesis*, 2003, 1541–1544.
58 G. Ginocchietti, G. Galiazzo, U. Mazzucato and A. Spalletti, *Photochem. Photobiol. Sci.*, 2005, **4**, 547–553.
59 F. Terenziani, A. Painelli, C. Katan, M. Charlot and M. Blanchard-Desce, *J. Am. Chem. Soc.*, 2006, **128**, 15742–15755.
60 E. Lippert, *Z. Naturforsch., A: Astrophys. Phys. Phys. Chem.*, 1955, **10**, 541–545.
61 N. Mataga, Y. Kaifu and M. Koizumi, *Bull. Chem. Soc. Jpn.*, 1955, **28**, 690–691.
62 J. R. Lakowicz, *Principles of Fluorescence Spectroscopy*, Kluwer Academic/Plenum Publishers, 1999.
63 C. Flors, P. R. Ogilby, J. G. Luis, T. A. Grillo, L. R. Izquierdo, P.-L. Gentili, L. Bussotti and S. Nonell, *Photochem. Photobiol.*, 2006, **82**, 95–103.
64 P. R. Ogilby, *Chem. Soc. Rev.*, 2010, **39**, 3181–3209.
65 C. Xu and W. W. Webb, *J. Opt. Soc. Am. B*, 1996, **13**, 481–491.
66 M. Lal, L. Levy, K. S. Kim, G. S. He, X. Wang, Y. H. Min, S. Pakatchi and P. N. Prasad, *Chem. Mater.*, 2000, **12**, 2632–2639.
67 S. Kim, H. Huang, H. E. Pudavar, Y. Cui and P. N. Prasad, *Chem. Mater.*, 2007, **19**, 5650–5656.
68 D. R. Larson, H. Ow, H. D. Vishwasrao, A. A. Heikal, U. Wiesner and W. W. Webb, *Chem. Mater.*, 2008, **20**, 2677–2684.
69 V. Lebret, L. Raehm, J.-O. Durand, M. Smaïhi, C. Gérardin, N. Nerambourg, M. H. V. Werts and M. Blanchard-Desce, *Chem. Mater.*, 2008, **20**, 2174–2183.
70 D. Gao, R. R. Agayan, H. Xu, M. A. Philbert and R. Kopelman, *Nano Lett.*, 2006, **6**, 2383–2386.
71 M. Velusamy, J.-Y. Shen, J. T. Lin, Y.-C. Lin, C.-C. Hsieh, C.-H. Lai, C.-W. Lai, M.-L. Ho, Y.-C. Chen, P.-T. Chou and J.-K. Hsiao, *Adv. Funct. Mater.*, 2009, **19**, 2388–2397.
72 D. F. Eaton, *Pure Appl. Chem.*, 1988, **60**, 1107–1114.
73 J. N. Demas and G. A. Crosby, *J. Phys. Chem.*, 1971, **75**, 991–1024.
74 M. A. Albota, C. Xu and W. W. Webb, *Appl. Opt.*, 1998, **37**, 7352–7356.
75 M. H. V. Werts, N. Nerambourg, D. Pélégry, Y. Le Grand and M. Blanchard-Desce, *Photochem. Photobiol. Sci.*, 2005, **4**, 531–538.
76 C. Katan, S. Tretiak, M. H. V. Werts, A. J. Bain, R. J. Marsh, N. Leonczek, N. Nicolaou, E. Badaeva, O. Mongin and M. Blanchard-Desce, *J. Phys. Chem. B*, 2007, **111**, 9468–9483.
77 R. Schmidt and E. Afshari, *J. Phys. Chem.*, 1990, **94**, 4377–4378.

